Penerbit UTHM

IJIE

Journal homepage: http://penerbit.uthm.edu.my/ojs/index.php/ijie
ISSN : 2229-838X e-ISSN : 2600-7916

The International Journal of Integrated Engineering

Fabrication and Experimental Evaluation of Simple Tissue-Mimicking Phantoms with Realistic Electrical Properties for Impedance-Based Sensing

J. Liu[1]*, C. Goehring[1], F. Schiele[2], K. Moeller[3], P. P. Pott[1]

[1]Institute of Medical Device Technology,
University of Stuttgart, Stuttgart, GERMANY

[2]Institute of Design and Production in Precision Engineering,
University of Stuttgart, Stuttgart, GERMANY

[3]Institute of Technical Medicine (ITeM),
Furtwangen University, Villingen-Schwenningen, GERMANY

*Corresponding Author

DOI: https://doi.org/10.30880/ijie.2021.13.05.014
Received 15 April 2021; Accepted 23 May 2021; Available online 31 July 2021

Abstract: Venipuncture is one of the most often performed invasive clinical procedure. Nevertheless, complications still occur. One opportunity to counteract these complications is to indicate the insertion by electrical impedance measurement, which bases on the various electrical properties of different tissues. This paper presents the evaluation and reproducible fabrication of simple tissue-mimicking phantoms for investigation of impedance sensing techniques. Three different tissue-mimicking phantoms, representing blood, fat, and skin, were made on water-based recipes, including agar and gelatin as gelling agents. For evaluation of the electrical properties an electrode probe, made of hypodermic needles, was fabricated and characterized using six sodium chloride (NaCl) solutions of defined concentrations. For characterization of the phantoms, conductances were measured over a frequency range from 20 Hz up to 1 MHz using the self-fabricated electrodes. The calculated conductivities of the tissue-mimicking phantoms showed sufficient agreement with corresponding electrical literature data of native tissue. Tests with a layered tissue structure proved usability for impedance-based venous entry tests. However, the method proposed was not suitable for investigation of relative permittivity, which would be required for full electrical characterization.

Keywords: Venipuncture, tissue-mimicking phantom, impedance measurement

1. Introduction

Venipuncture, the process of getting access to a superficial vein by injecting a hollow needle, is one of the most performed clinical interventions. It is used to draw blood from or administer solutions or medications into the bloodstream [1], [2]. In general, the puncture procedure is performed by a clinician, who uses a tourniquet to limit the blood flow inside the vessel for a better identification of the target vein. Right after disinfecting the skin, the needle is inserted into the target vein and the correct implementation is recognized through a flashback of blood into the cannula [3]. Therefore, a painless and effective venipuncture depends on the skills and level of experience of the healthcare professional. Furthermore, the anatomy, skin color, and the physiological conditions of the patient, affected by age, adiposity, or pre-existing diseases, can compromise the venipuncture [4]. Possible complications can occur if

*Corresponding author: jan.liu@imt.uni-stuttgart.de

the needle is inserted only partially into the vessel or if the vein is completely pierced. Leakage of blood and hematomas are considered main consequences [5].

There are different ways to counteract these complications and to facilitate the process of venipuncture for the clinician. The most common approaches deal with measurement of the insertion force during insertion [6], [7] or with an investigation of the electrical impedance of tissues [8]. The indication of a correct venipuncture by measuring the electrical impedance is based on the electrical properties of biological structures, which vary by the amount of water, cell type and composition of the target tissue [9]. These properties can be influenced by the physiological condition of the patient such as age or changes due to previous diseases. For electrical characterization of different tissues, samples from biopsies are often used. However, excised tissue samples, in many cases, exhibit different amounts of water, which influences the electrical properties in a considerable way. Furthermore, the availability of target tissue samples can be problematic [10]. Therefore, a simple process to manufacture tissue phantoms with realistic electrical properties is desired for the investigation and development of impedance sensing techniques.

In case of venipuncture, the phantoms should primarily represent the properties of skin and blood to indicate the insertion of the needle into the vein. Distinction of these biological tissue types are based on the large variety in conductivity. In general, tissue is a very heterogeneous material, which is considerably influenced by boundary processes. Therefore, the electrical properties exhibit frequency dependence, and anisotropy. The skin itself consists of three different layers, which differ in conductivity due to different cell types, structure, and composition [9]. The epidermis is the surficial layer of the skin and is strongly insulating electrically. The underlying dermis is a compressible and elastic connective tissue which mainly influences the mechanical properties of the skin [11]. Compared to the epidermis, with a conductivity between 10-7 to 10–4 S/m (depending on frequency) [9], the dermis is a much better conductor with an averaged conductivity of approximately 0.25 S/m in a frequency range of 20 Hz up to 1 MHz [12]. The veins for venipuncture are located in the area of the lowest skin layer, the subcutis. This part of the skin is an adipose layer and separates the skin from the underlying tissues [11]. Because of the low amount of water in the subcutis, the conductivity is approximately 0.04 S/m in a frequency range of 10 Hz up to approximately 1 MHz [9], [13]. In contrast to the different layers of skin, blood contains better conductive properties related to electrically charged molecules, which induce an averaged conductivity of approximately 0.7 S/m [9].

To simulate the outlined properties of different tissues at various frequencies, diverse tissue-mimicking phantom materials have been investigated and described in literature. Most of them were used to examine the interaction of electromagnetic waves with biological tissues. These materials can be categorized by reference to their main ingredient [14]. One of the earliest reports by Guy in 1971 comprises the use of sodium chloride (NaCl), polyethylene powder and a gelling agent to simulate muscle. Furthermore, Guy utilized polyester resin, acetylene black and aluminum powder for development of fat and bone phantoms in a frequency range of 433 up to 2450 MHz [15].

A completely different approach was tested by Bini et al. and Andreuccetti et al. [16], [17]. They used polyacrylamide in combination with NaCl to adjust the conductivity for different tissue-mimicking phantoms. Polyacrylamide is advantageously because of its optical transparency and mechanical properties, but the fabrication is linked to complicated processes and chemicals that are difficult to access [16], [17]. Another class of materials, which were already used for tissue-mimicking phantoms, includes carbon in combination with an insulating matrix. Silicones with various amounts of graphite were used by Gabriel to generate hand phantoms [18]. Garrett and Fear studied the usage of graphite and carbon black in combination with urethane as matrix material to fabricate different soft tissue-mimicking phantoms in a frequency range from 1 up to 10 GHz. However, the samples were not mechanically suitable for modelling complex geometries [19].

Phantoms, which base on gelatin or agar are favorable because of their stable mechanical properties, almost unfettered shaping, and easy fabrication. In general, they are water-based, with gelatin or agar as gelling agent. Furthermore, they contain NaCl to adjust conductivity, sucrose or polyethylene to adjust permittivity, and a preservative [20]–[22]. These ingredients enable simple and low-cost manufacturing of different tissue phantoms like brain [20], breast [23], or muscle [22]. For example, Yu et al. investigated the electrical and mechanical properties of muscle-mimicking phantoms in a frequency range of 20 Hz to 100 kHz using gelatin and agar powder in combination with NaCl, glycin and aluminum powder [22]. Moreover, Anand et al. did not only use agar-based phantoms to simulate soft tissues, they also investigated different solutions for mimicking the electrical properties of blood [24].

Based on these findings, gelatin and agar should be used for creating different tissue-mimicking phantoms to simulate electrical properties for tissues involved in the process of venipuncture. Moreover, the aim is to create and fabricate phantoms in a simple way with ingredients available off-the-shelf. The fabrication and measurement method should be reproducible to establish a procedure for evaluation of electric impedance sensing techniques.

2. Materials and Methods

2.1 Target Properties

During venipuncture, the cannula permeates the epidermis, dermis, subcutis, and vascular wall until it reaches venous blood. This work focuses on the fabrication of dermis-, fat-, and blood-mimicking phantoms. As already

mentioned above, the approximately target conductivities are 0.25 S/m for dermis-[12], 0.04 S/m for fat-, and 0.7 S/m for blood-mimicking phantoms [9].

2.2 Process of Phantom Fabrication

The ingredients used for phantom fabrication are mainly based on Anand et al. [24]. Therefore, agar, NaCl, gelatin, propylene glycol, and demineralized water were the main ingredients used (VWR International LLC, Radnor, Pennsylvania, US).

For fabrication of the fat-mimicking phantom, hereinafter simply called fat phantom, the amount of demineralized water and agar, according to Table 1, was weighed using a precision scale (SBS-LW-200A, Steinberg Systems, Berlin, DE). Afterwards, the water was heated to 50 °C by using a magnetic stirrer hot plate with a flea (SBS-MR-1600/1T, Steinberg Systems, Berlin, DE), and the agar was added. In order to reach a good solubility, the solution was boiled for a moment. Meanwhile, it was covered with a glass lid to prevent loss of water. Finally, the solution was cooled down in a vacuum desiccator (DURAN DN250, DWK Life Sciences GmbH, Wertheim/Main, DE) for 70 s after the flea was removed. This ensured that the solution did not exhibit any air bubbles, and the temperature was still high enough to pour it in the preferred shape. After creating the final shape, illustrated in Fig. 1, the solution was settled down to room temperature (RT) before measurement.

For production of the dermis-mimicking phantom, hereinafter called skin phantom, the basic steps of the fat-mimicking phantom were repeated. After heating the water, NaCl was added and mixed until it was fully solved. Furthermore, the right amount of gelatin was added and solved before agar was eventually added.

A blood-mimicking phantom was created by mixing a solution of 30 % of 5 M NaCl and 70 % of propylene by weight.

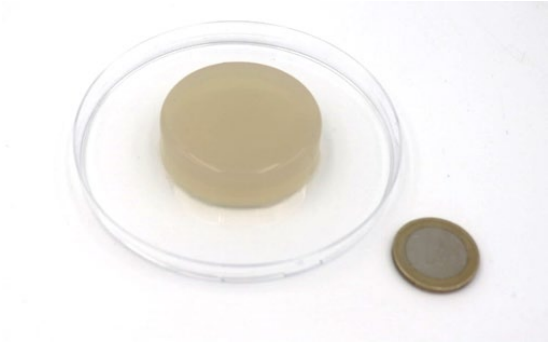

Fig. 1 - Fabricated fat phantom using demineralized water and agar. Diameter 4.5 cm, height 0.8 cm

Table 1 - Ingredients for phantom fabrication

Phantom type	Ingredients (% w/w)					
	Demineralized water	Sodium chloride (NaCl)	Agar	Gelatin	Propylene glycol	5 M NaCl solution
Skin	75.40	0.30	3.77	1.88	18.72	-
Fat	95.24	-	4.76	-	-	-
Blood	-	-	-	-	70.00	30.00

2.3 Characterization of Tissue-Mimicking Phantoms

2.3.1 Electrode Properties

The measurements to determine the electric properties of the phantoms were performed using a four-electrode method [25]. The electrodes were made of four 22 Gauge (G) hypodermic needles (B. Braun AG, Melsungen, DE) with an outer diameter of 0.7 mm and a length of 40 mm (Fig. 2). A bracket for defined distance between the single electrodes was fabricated by FDM 3D-printing. The distance between each electrode was 2.3 mm. Before inserting the hypodermic needles into the bracket, they were cut at the end and scratched using sandpaper to minimize their interface impedance. In a further step, to connect the electrodes, 40 cm of coaxial cable (RG58 50 Ohm, Klaus Faber AG, Saarbrücken, DE) was used for each electrode. At one side, the cables ends were stripped and soldered to the needles.

At the other side, BNC connectors were crimped to the coaxial cables. In order to isolate the soldering joints, shrinking tubes were applied. Finally, each needle was inserted into the bracket. The lengths of the exposed ends were 5.5 mm each. To keep the electrodes in position, cyanacrylate was used. The electrode head and the entire electrode probe are shown in Fig. 2.

For the investigation of the electrical properties of tissues, an alternating current or voltage can be applied. The resulting impedance Z is defined as:

$$Z = R + jX \tag{1}$$

where R is the resistance, X is the reactance, and j is the imaginary number $\sqrt{-1}$. Alternatively, it is possible to use the admittance Y, which is defined as follows:

$$Y = G + j\omega C \tag{2}$$

where C is the capacity, G the conductance, and $\omega = 2\pi f$ the angular frequency [13], [26], [27]. Moreover, the value G is depending on the sample properties and the geometry of the measurement system:

$$G = \sigma \frac{A}{d} = \sigma K \tag{3}$$

where σ is the conductivity (expressed in S/m), A is the electrode surface, d is the electrode length, and K is the cell constant which describes the ratio of surface to length (expressed in m). The conductance G (and the susceptance B) can be calculated using the measured resistance R (real part of impedance) and the measured reactance X (imaginary part of impedance):

$$G = \frac{R}{R^2+X^2} \cdot B = \frac{-X}{R^2+X^2} \tag{4}$$

To calculate the cell constant of the self-fabricated electrode probe, a method described by Gabriel et al. was used [28]. Therefore, solutions with sodium chloride (NaCl) concentrations of 0.001 M, 0.005 M, 0.01 M, 0.03 M, 0.05 M, and 0.15 M (VWR International LLC, Radnor, Pennsylvania, US) were mixed. The respective conductivity of each solution is given by a polynomial equation derived from experimental data [29]:

$$\sigma = 0.174TC - 1.582C^2 + 5.923C \tag{5}$$

where T is the temperature of the solution in °C and C is the concentration of the solution in mol/L. The conductivities of the NaCl solutions do not vary with frequencies below 1 MHz [28]. Using known conductivity values in combination with conductance measurements, enables the calculation of the cell constant K, according to equation (3) [29]. The found cell constants are further used to calculate unknown conductivity values for the fabricated tissue phantoms (see Fig. 3).

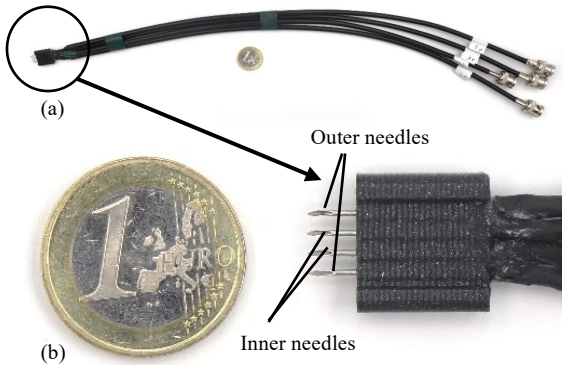

Fig. 2 - Four-electrode setup to measure electrical properties of the phantoms (a) Entire electrode probe; (b) head of the electrode probe

2.3.2 Measurement Settings

All measurements were performed using the self-fabricated electrode probe and a precision impedance analyzer (6500B, Wayne Kerr Electronics Inc., Woburn, US). In the following, the precision impedance analyzer will be referred to as PIA. The outer needles, show in Fig. 2 (b), were connected to the current outputs, and the inner needles were connected to the voltage sensing ports of the PIA. The excitation amplitude was set to 200 µA and the frequency ranged from 20 Hz to 1 MHz with 100 measurement points in logarithmic sequence. Each sample was measured three times in a row.

To simulate the process of venipuncture, tests were conducted in the following way. A layered structure was constructed with skin as the uppermost layer, followed by fat, both lying on a reservoir filled with the blood-mimicking fluid. A universal testing machine (QUASAR 25, Cesare Galdabini SPA, Cardano al Campo, IT) is used for inserting a handheld impedance measurement device into the different layers of tissue phantoms with a constant velocity of 1 mm/s (Fig. 3). In contrast to the work presented in this paper, the handheld impedance measurement device uses a two-electrode setup, consisting of two hypodermic needles, separated by an insulating layer of PTFE (Fig. 4). This setup enables impedance measurements for insertions with increased insertion depths. The handheld device incorporates a Pmod impedance analyzer (Diligent Inc., Pullman, Washington, US) with an AD5933 impedance analyzer chip (Analog Devices Inc., Norwood, Massachusetts, US), controlled by an Arduino Nano (Arduino LLC, Somerville, Massachusetts, US). To find a set test frequency that is suitable for the insertion tests, the conductivity values from the PIA are compared against values found using the handheld impedance measurement device. Using a digital caliper, the layer thicknesses of the phantoms were measured to be approximately 8 mm. Only an approximate value can be given as the layer thickness is not always constant due to the fabrication process. The insertion process was performed 10 times at varying locations.

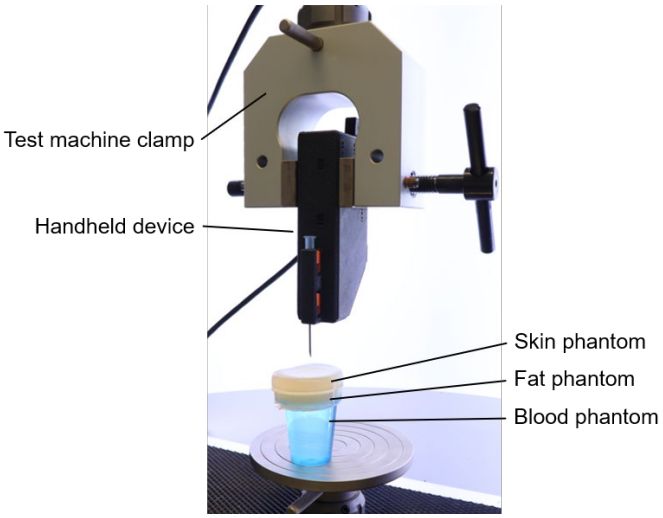

Fig. 3 - Measurement setup for determining conductivities during insertion into the layered tissue phantom. The handheld device is clamped by the test machine and inserted into the tissue phantoms with a constant velocity of 1 mm/s

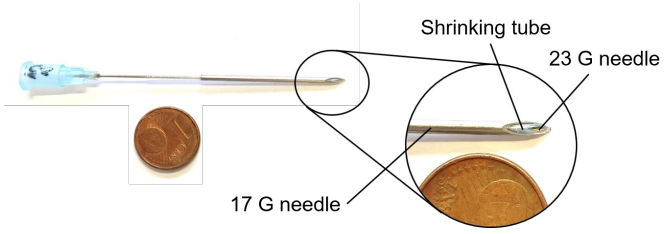

Fig. 4 - Two-electrode setup to measure electrical properties of the phantoms

3. Results

3.1 Cell Constant

Fig. 5 illustrates the measured conductances for the NaCl solutions with concentrations from 0.001 M to 0.15 M in a frequency range from 20 Hz up to 1 MHz, using the four-electrode probe (Fig. 2). It is clearly discernible that the conductance increases with the concentration. Each curve shows a nearly constant behavior over the whole frequency

range, expect for 0.001 M. Values for high frequencies, which are not represented for 0.001 M curve, turned even negative. The evaluation of the recorded data is shown in Table 2. Conductivity literature values from Peyman et al. [29] and averaged conductance over the whole frequency range were used to calculate the cell constant of the electrode according to equation (3). Table 2 displays a percentual difference of 19.60 % for the 0.001 M solution. Therefore, the values of this solution were disregarded for calculation of the cell constant. Considering this, the averaged cell constant from the remaining five NaCl solutions results in 0.173 m. Furthermore, it can be seen that, for solutions from 0.005 M to 0.15 M, the difference was below 5 %.

Table 2 - Evaluation of calculated conductivity of tissue-mimicking phantoms

NaCl concentration (M)	G (S) average	G (S) standard deviation	G (S) standard deviation	σ (S/m) calculated	σ (S/m) Peyman et al. [29]	σ (S/m) difference	K (m)
0.001	1.25E-03	1.60E-03	127.54 %	0.007	0.009	-19.60 %	0.139
0.005	8.31E-03	6.23E-04	7.51 %	0.048	0.047	2.02 %	0.177
0.01	1.66E-02	1.20E-03	7.24 %	0.096	0.094	2.09 %	0.177
0.03	4.88E-02	4.07E-03	8.33 %	0.282	0.281	0.20 %	0.174
0.05	7.71E-02	7.79E-03	10.10 %	0.445	0.466	-4.53 %	0.165
0.15	2.39E-01	2.61E-02	10.94 %	1.378	1.375	0.22 %	0.174

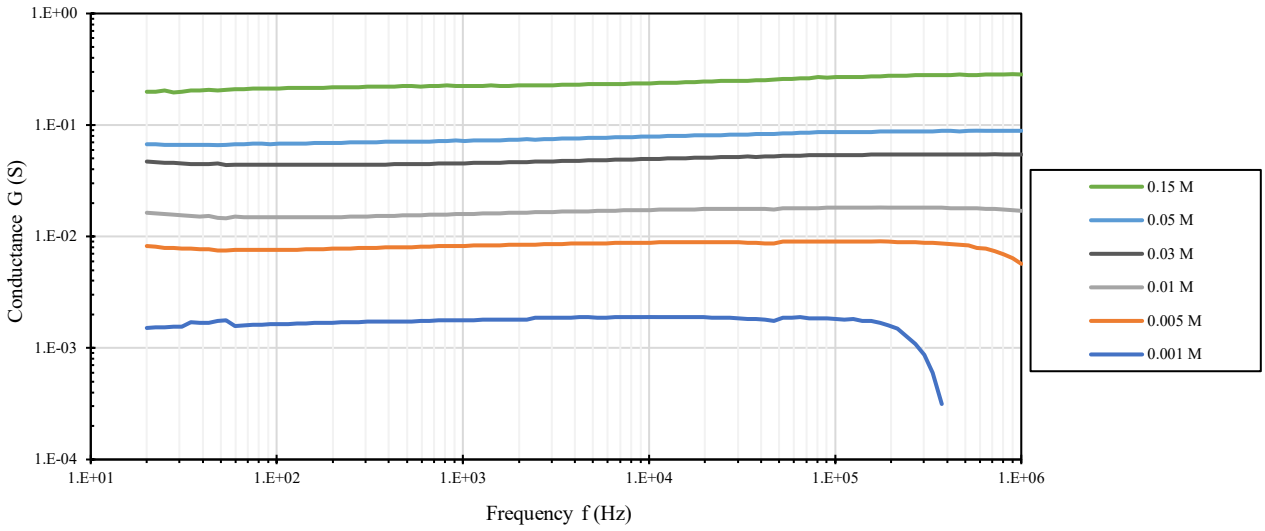

Fig. 5 - Conductance G (S) of NaCl solutions depending on concentration (see Table 2) to calculate the cell constant of the four-electrode probe (see Fig. 2)

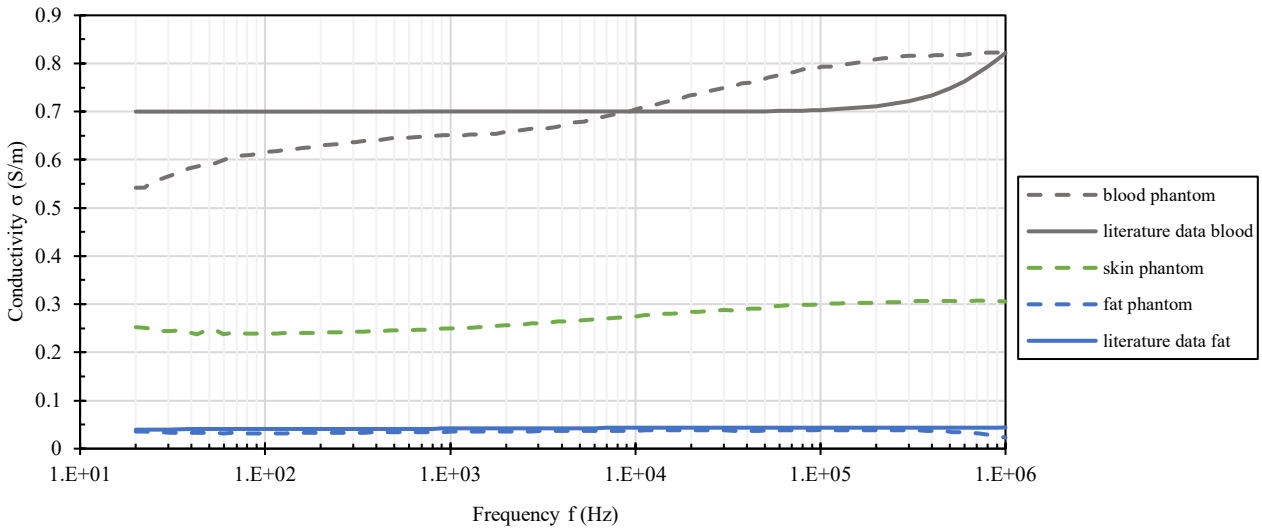

Fig. 6 - Calculated conductivities of three different tissue-mimicking phantoms (n = 3) using measured conductances and calculated cell constant. Additionally, literature data for fat and blood, according to Gabriel et al. is illustrated [28], [30]–[35]

3.1.1 Electrical Characterization of Phantom Tissues

Fig. 6 shows the calculated conductivity values for each tissue-mimicking phantom, using the measured conductance and the calculated cell constant (0.173 m) according to equation (3), and corresponding literature values for blood and fat from Gabriel et al. [28], [30]–[35]. Each phantom was fabricated three times. The calculated conductivity values are expressed as an average of the three replicas, and Table 3 evaluates the average values. The differences from the target values are below 13.50 %.

With the determined cell constant for the bipolar two-electrode probe (3.72 · 10-3 m), conductivities found using the Pmod impedance analyzer were derived for the fabricated tissue phantoms. Fig. 7 (a) shows the conductivities of blood and fat according to Gabriel et al. [30], the conductivities found using the precision impedance analyzer, and the conductivities determined by the Pmod. It can be seen that, for the fat phantom (yellow lines), the conductivities determined by both devices are nearly constant and show little absolute deviations from the literature value (0.04 S/m). The average relative error is 4.68 % for the PIA, and 26.83 % for the Pmod. The conductivity values for the blood phantom (blue lines) increase strongly as the frequency increases. In the frequency range observed, the data from the PIA is always above the literature values, whereas the data from the Pmod is slightly below, reaching the targeted literature value (0.07 S/m) at a frequency of 100 kHz. The average relative error in respect to the literature value is 9.13 % for the PIA, and 18.11 % for the Pmod. For the skin phantom (orange lines), frequency-dependent conductivity values were not found that solely regard the properties of the dermis without considering the epidermis with its strongly insulating stratum corneum, dominating the electrical properties of skin. However, an averaged constant conductivity can be given as 0.25 S/m [12]. Recorded conductivity values by the Pmod start matching the PIA values, which are slightly above the targeted skin phantom conductivity, from roughly 70 kHz on. The average relative error is 16.89 % for the PIA, and 13.13 % for the Pmod.

Table 3 - Evaluation of calculated conductivity of tissue-mimicking phantoms using the four-electrode probe

Phantom	G (S) average	σ (S/m) calculated	σ (S/m) target value	σ (S/m) difference
Blood	1.20E-01	0.697	0.7	-0.43 %
Skin	4.67E-02	0.270	0.25	7.37 %
Fat	6.12E-03	0.035	0.04	-13.18 %

3.1.2 Venous Entry Test

As the greatest accordance between PIA and Pmod (~ 15 % difference), and the conductivity values from the Pmod and literature values (~17 % difference), is observed for a frequency of 100 kHz, this is used for evaluating the

functionality with a layered phantom structure. In Fig. 7 (b), a plot can be seen displaying the mean conductivity and the standard deviation as error bars. As the uppermost skin layer is reached and pierced after a travel distance of 3 mm, the conductivity rises to approximately 0.25 S/m. The needle is further advanced and reaches the fat layer after travelling roughly 11 mm, visible as a drop in conductivity to around 0.06 S/m. Blood contact is established after a travel distance of approximately 19 mm, indicated by a rise in conductivity. By setting an internal threshold, it is now possible to light up the integrated LED, signalizing the performing clinician that a specific target structure has been reached.

4. Discussion

The measured conductance values of the NaCl solutions (see Fig. 5) show no variation with frequency as presumed [28]. Moreover, the presented results for cell constant calculation in Table 2 also show very small differences, smaller than previously reported, e. g., 2.02 % deviation for the 0.005 M solution, compared to 8.42 % (Laufer et al.) or 10.05 % (Gabriel et al.) [25], [28]. For 0.001 M, a higher error in general was detected. Here, a percentual deviation of 19.60 % was calculated, compared to 25.82 % (Laufer et al.) and 67.15 % (Gabriel et al.) [25], [28]. Therefore, the values of this solution were disregarded for calculation of the cell constant. Additionally, these data are not relevant to describe the range of body tissues and fluids conductivity [28]. Nevertheless, the curves of literature data for blood and fat, displayed in Fig. 6, are close to the calculated values. Furthermore, an evaluation of the average values of all fabricated phantoms, presented in Table 3, shows that the target conductivities are successfully met. Despite the fact that the measurements were carried out at a slightly higher temperature than 20 °C which the data by Peyman et al. is based on, the method is very suitable to determine properties of electrodes [29]. By knowing the cell constant, it was possible to determine the conductivity of the tissue-mimicking phantoms fabricated. Investigation and determination of relative permittivities cannot be achieved with this method. This is due to large noise when measuring the capacity with the impedance analyzer. Capacity measurements are highly effected by electrode polarization and need a different electrode design [28].

It is further worth mentioning that, when transitioning between two layers, a mixed conductivity of both layers is measured as both electrodes of the two-electrode probe are still partly in the previous layer. When both electrodes are within the same layer, the measured impedance is constant and does not change with further insertion within this layer. In Fig. 7 (b), where the conductivity value does not change instantly, but gradually, this effect is visualized. The effect is even enhanced as the measurement points depict the average out of 10 measurements, and the layers do not have constant thicknesses. Therefore, the travel distances inside the layers vary slightly, also increasing the standard deviation.

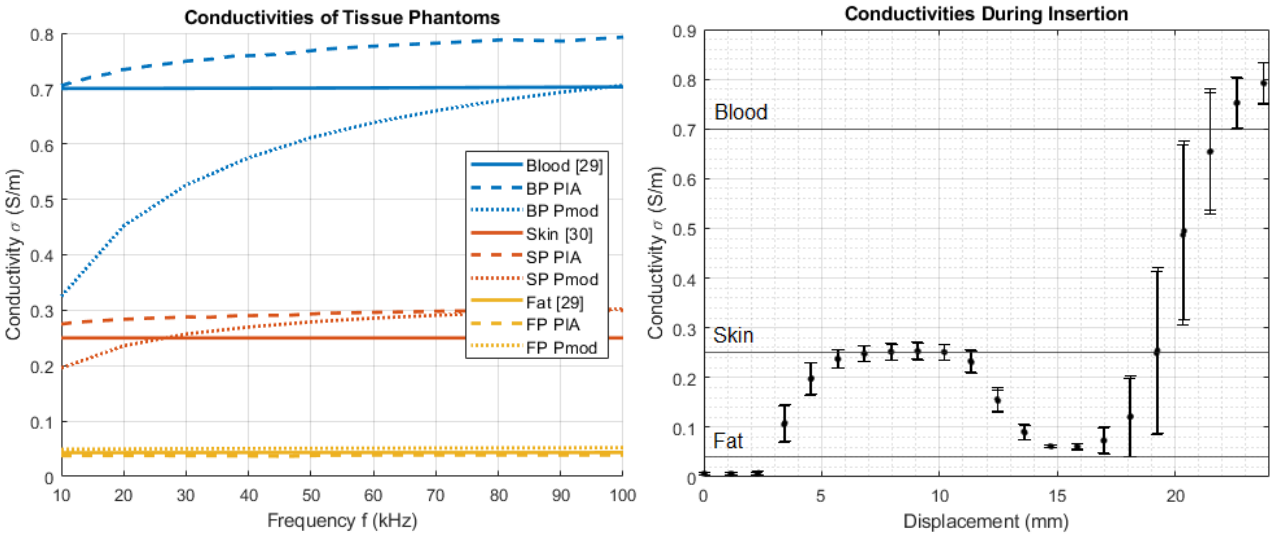

Fig. 7 - (a) Conductivities of various tissue phantoms (BP: blood phantom, SP: skin phantom, FP: fat phantom; PIA: precision impedance analyzer, Pmod: Pmod with AD5933); (b) Conductivities during insertion into a layered tissue phantom. The graph shows measurement points, averaging a total of 10 measurements. The error bars indicate the standard deviation

5. Conclusion

This paper describes a method to fabricate low-cost tissue-mimicking phantoms with realistic conductivities and how to characterize them using self-fabricated electrodes. Additionally, the manufacturing processes for both phantoms

and electrodes are simple and do not require extensive accessories. However, the method does not include relative permittivity which would be required for full electrical characterization of the tissue-mimicking phantoms. Because loss of water during storage of the phantoms could affect the electrical properties, a future investigation of the phantom properties over time is conceivable.

References

[1] Rickard, C. M., Webster, J., Wallis, M. C., Marsh, N., McGrail, M. R., French, V., et al. (2012). Routine versus clinically indicated replacement of peripheral intravenous catheters: a randomised controlled equivalence trial. The Lancet, 380(9847), 1066–1074

[2] Zingg, W., & Pittet, D. (2009). Peripheral venous catheters: an under-evaluated problem. International Journal of Antimicrobial Agents, 34, S38-S42

[3] Dhingra, N. (2010). WHO guidelines on drawing blood: Best practices in phlebotomy. Safe Injection Global Network, World Health Organization

[4] Helm, R. E., Klausner, J. D., Klemperer, J. D., Flint, L. M., & Huang, E. (2015). Accepted but unacceptable: Peripheral IV catheter failure. Journal of Infusion Nursing: The Official Publication of the Infusion Nurses Society, 38(3), 189–203

[5] Sorensen, B. S., Johnsen, S. P., & Jorgensen, J. (2008). Complications related to blood donation: A population-based study. Vox Sanguinis, 94(2), 132–137

[6] Zhuoqi, C., Chauhan, M., Davies, B. L., Caldwell, D. G., & Mattos, L. S. (2015). Modelling needle forces during insertion into soft tissue. Annual International Conference of the IEEE Engineering in Medicine and Biology Society. IEEE Engineering in Medicine and Biology Society. Annual International Conference, 2015, 4840–4844

[7] Zivanovic, A., & Davies, B. L. (2000). A robotic system for blood sampling. IEEE Transactions on Information Technology in Biomedicine, 4(1), 8–14

[8] Kalvoy, H., Martinsen, O. G., & Grimnes, S. (2008). Determination of tissue type surrounding a needle tip by electrical bioimpedance. Annual International Conference of the IEEE Engineering in Medicine and Biology Society, 2008, 2285–2286

[9] Grimnes, S., & Martinsen, Ø. G. (op. 2015). Bioimpedance and bioelectricity basics. Elsevier

[10] Geddes, L. A., & Baker, L. E. (1967). The specific resistance of biological material--a compendium of data for the biomedical engineer and physiologist. Medical & Biological Engineering, 5(3), 271–293

[11] Kanitakis, J. (2002). Anatomy, histology and immunohistochemistry of normal human skin. European Journal of Dermatology: EJD, 12(4), 390-9; quiz 400-1

[12] Yamamoto, T., & Yamamoto, Y. (1976). Electrical properties of the epidermal stratum corneum. Medical & Biological Engineering, 14(2), 151–158

[13] Miklavčič, D., Pavšelj, N., & Hart, F. X. (2006). Electric Properties of Tissues. In M. Akay (Ed.), Wiley Encyclopedia of Biomedical Engineering. John Wiley & Sons, Inc

[14] Lazebnik, M., Madsen, E. L., Frank, G. R., & Hagness, S. C. (2005). Tissue-mimicking phantom materials for narrowband and ultrawideband microwave applications. Physics in Medicine and Biology, 50(18), 4245–4258

[15] Guy, A. W. (1971). Analyses of Electromagnetic Fields Induced in Biological Tissues by Thermographic Studies on Equivalent Phantom Models. IEEE Transactions on Microwave Theory and Techniques, 19(2), 205–214

[16] Andreuccetti, D., Bini, M., Ignesti, A., Olmi, R., Rubino, N., & Vanni, R. (1988). Use of polyacrylamide as a tissue-equivalent material in the microwave range. IEEE Trans. Biomed. Eng., 35(4), 275–277

[17] Bini, M. G., Ignesti, A., Millanta, L., Olmi, R., Rubino, N., & Vanni, R. (1984). The polyacrylamide as a phantom material for electromagnetic hyperthermia studies. IEEE Trans. Biomed. Eng., 31(3), 317–322

[18] Gabriel, C. (2007). Tissue equivalent material for hand phantoms. Physics in Medicine and Biology, 52(14), 4205–4210

[19] Garrett, J., & Fear, E. (2014). Stable and Flexible Materials to Mimic the Dielectric Properties of Human Soft Tissues. IEEE Antennas and Wireless Propagation Letters, 13, 599–602

[20] Duan, Q., Duyn, J. H., Gudino, N., Zwart, J. A. de, van Gelderen, P., Sodickson, D. K., et al. (2014).Characterization of a dielectric phantom for high-field magnetic resonance imaging applications. Medical Physics, 41(10), 102303

[21] Mendes, C., & Peixeiro, C. (2019). Fabrication, Measurement and Time Decay of the Electromagnetic Properties of Semi-Solid Water-Based Phantoms. Sensors (Basel, Switzerland), 19(19)

[22] Yu, Y., Lowe, A., Anand, G., & Kalra, A. (2019). Tissue phantom to mimic the dielectric properties of human muscle within 20 Hz and 100 kHz for biopotential sensing applications. Annual International Conference of the IEEE Engineering in Medicine and Biology Society. IEEE Engineering in Medicine and Biology Society. Annual International Conference, 2019, 6490–6493

[23] Mashal, A., Gao, F., & Hagness, S. C. (2011). Heterogeneous Anthropomorphic Phantoms with Realistic Dielectric Properties for Microwave Breast Imaging Experiments. Microwave and Optical Technology Letters, 53(8), 1896–1902

[24] Anand, G., Lowe, A., & Al-Jumaily, A. (2019). Tissue phantoms to mimic the dielectric properties of human forearm section for multi-frequency bioimpedance analysis at low frequencies. Materials Science & Engineering. C, Materials for Biological Applications, 96, 496–508
[25] Laufer, S., Ivorra, A., Reuter, V. E., Rubinsky, B., & Solomon, S. B. (2010). Electrical impedance characterization of normal and cancerous human hepatic tissue. Physiological Measurement, 31(7), 995–1009.
[26] Reilly, J. P. (1998). Applied Bioelectricity. Springer New York
[27] Schwan, H. P. (1957). Electrical properties of tissue and cell suspensions. Advances in Biological and Medical Physics, 5, 147–209
[28] Gabriel, C., Peyman, A., & Grant, E. H. (2009). Electrical conductivity of tissue at frequencies below 1 MHz. Physics in Medicine and Biology, 54(16), 4863–4878
[29] Peyman, A., Gabriel, C., & Grant, E. H. (2007). Complex permittivity of sodium chloride solutions at microwave frequencies. Bioelectromagnetics, 28(4), 264–274
[30] Gabriel, C. (1996). Compilation of the Dielectric Properties of Body Tissues at RF and Microwave Frequencies. Final Technical Report. Fort Belvoir, VA. US Air Force
[31] Gabriel, C., Gabriel, S., & Corthout, E. (1996). The dielectric properties of biological tissues: I. Literature survey. Physics in Medicine and Biology, 41(11), 2231–2249
[32] Gabriel, S., Lau, R. W., & Gabriel, C. (1996). The dielectric properties of biological tissues: Ii. Measurements in the frequency range 10 Hz to 20 GHz. Physics in Medicine and Biology, 41(11), 2251–2269
[33] Gabriel, S., Lau, R. W., & Gabriel, C. (1996). The dielectric properties of biological tissues: Iii. Parametric models for the dielectric spectrum of tissues. Physics in Medicine and Biology, 41(11), 2271–2293
[34] Peyman, A., & Gabriel, C. (2010). Cole-Cole parameters for the dielectric properties of porcine tissues as a function of age at microwave frequencies. Physics in Medicine and Biology, 55(15), N413-9
[35] Peyman, A., & Gabriel, C. (2012). Dielectric properties of porcine glands, gonads and body fluids. Physics in Medicine and Biology, 57(19), N339-44